RSC Advances

ROYAL SOCIETY OF CHEMISTRY

www.rsc.org/advances

Mesostructure-tunable and size-controllable hierarchical porous silica nanospheres synthesized by aldehyde-modified Stöber method

Anfeng Zhang[a], Lin Gu[b], Keke Hou[c], Chengyi Dai[a], Chunshan Song[a,d*] and Xinwen Guo[a] *

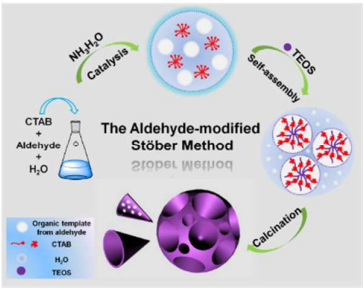

Mesostructure-fine-tuned and size-controlled hierarchical porous silica nanospheres were synthesized by aldehyde-modified Stöber method in the TEOS-CTAB-NH_3•H_2O-aldehyde system.

RSC Advance

PAPER

Mesostructure-tunable and size-controllable hierarchical porous silica nanospheres synthesized by aldehyde-modified Stöber method

Received 00th January 20xx,
Accepted 00th January 20xx

DOI: 10.1039/x0xx00000x

www.rsc.org/

Anfeng Zhang[a], Lin Gu[b], Keke Hou[c], Chengyi Dai[a], Chunshan Song[a,d*] and Xinwen Guo[a] *

Mesostructure-fine-tuned and size-controlled hierarchical porous silica nanospheres were synthesized by aldehyde-modified Stöber method in the TEOS-CTAB-NH_3•H_2O-aldehyde system. The samples were characterized by XRD, N_2 adsorption-desorption isotherms, SEM, TEM and TG analysis. The results indicate that the particle size of the micro/mesoporous silica nanospheres synthesized with acetaldehyde as a co-solvent can be controlled from 40 to 850 nm by regulating the molar ratio of acetaldehyde to water and the initial pH of the synthesis solution. When propionaldehyde or butyraldehyde was used as a co-solvent, hierarchical porous silica nanospheres with large cone-like cavities and small mesopores in the cavity wall were synthesized; the diameter of the flower-like nanospheres is less than 130 nm. The hierarchical pore structure of the flower-like silica nanospheres can be fine-tuned by controlling the polymerization of butyraldehyde by the synthesis temperature from 27 to 100 °C, both the depth and opening diameter of the cone-like cavities can be fine-tuned from 40 to 2 nm; simultaneously, the small mesopores templated by CTAB become more ordered.

Introduction

Mesoporous materials with a defined morphology and topology are of interest for various applications including adsorption[1-4], catalysts[5-7], drug delivery[8, 9] and controlled release[10]. Among the defined morphologies, size-controlled mesoporous silica spheres are particularly important for fundamental science and the potential applications[11-13]. Several direct methods have been developed to synthesize mesoporous silica spheres using surfactants as templates for mesopores during the spheres formation. To control the particle size and monodispersity, growth inhibitor additives, such as formaldehyde[14], triblock copolymer[15], triethanol amines[16, 17], and functional organosilanes[18, 19] have been used to improve the synthesis process, resulting in better control of particle size. Monodisperse mesoporous silica nanospheres can also be produced under kinetic control using dilution and acid quenching[20, 21]. For the synthesis of sillica spheres, the well-established Stöber method yields products with controllable size and high monodispersity[22]. To introduce mesopores into Stöber spheres, surfactant-induced pseudomorphic transformations have been reported[23-25], which provides an alternative method to direct synthesis of mesoporous silica nanospheres. However, to control the particle size smaller than 200 nm and regulate the pore structure simultaneously is still a major challenge.

Recently, hierarchical porous silica nanospheres with radial-oriented mesochannels and a conical pore shape, have become attractive for its special flower-like morphology and hierarchical pore structure, which greatly benefit the accessibility of large molecules[26-28]. Several groups have synthesized the flower-like mesoporous silica nanospheres using microemulsion media[29-31]. By the simultaneous hydrolytic condensation of tetraorthosilicate to form silica and polymerization of styrene into polystyrene, Nandiyanto prepared spherical mesoporous silica particles with conical pores and tunable outer particle diameter[29]. Polshettiwar reported the synthesis of silica nanospheres with dendrimeric fibers using cyclohexane and pentanol as co-solvent[30]. To synthesize the flower-like silica nanospheres with hierarchical pore structure, mesopore structure directing agent and organic co-solvent were introduced. Using cetyltrimethyl ammonium chloride as structure-directing agent, and the mixture of ethyl ether and water as solvent, Zhang prepared chrysanthemum-like mesoporous silica nanoparticles which exhibited excellent controlled release performance for pyrene[7]. Large-scale synthesis of flower-like nanospheres was realized using cetyltrimethylammonium tosylate as a template, and with small organic amines as co-solvent[32]. Recently, flower-like silica nanospheres with hierarchical micro–meso–macro porous structures were synthesized using cetylpyridinium bromide as the template,

[a] State Key Lab of Fine Chemicals, PSU-DUT Joint Center for Energy Research, School of Chemical Engineering, Dalian University of Technology, Dalian 116024, P R. China. Fax: 86-0411-86986134; Tel: 86-0411-86986133; E-mail: Guoxw@dlut.edu.cn
[b] Shanghai Baosteel Chemical Co., Ltd. No.3501 Tongji Road, Shanghai, P R. China.
[c] Chambroad Chemical Industry Research Institute Co.,LTD, Binzhou, Shandong, P R. China.
[d] EMS Energy Institute, PSU-DUT Joint Center for Energy Research, Department of Energy & Mineral Engineering, and Department of Chemical Engineering Pennsylvania State University, University Park, Pennsylvania 16802, United States. Fax: 814-865-3573; Tel: 814-863-4466; E-mail: csong@psu.edu
Electronic Supplementary Information (ESI) available: [details of any supplementary information available should be included here]. See DOI: 10.1039/x0xx00000x

cyclohexane and pentanol as co-solvent[33]. Up to now, only a few literatures present the synthesis of hierarchical porous silica nanospheres with flower-like morphology, the fine tuning of the hierarchical pore structure still remains a great challenge.

Herein, by the simultaneous hydrolytic condensation of tetraorthosilicate to form silica and the polymerization of aldehyde into polymers, we successfully synthesized size-controlled micro/mesoporous silica nanospheres, and hierarchical porous silica nanospheres with large cone-like cavities and small mesopores in the cavity wall by the aldehyde-modified Stöber method. Taking advantage of the temperature-sensitive polymerization of aldehyde during the synthesis process, the hierarchical pore structure of the flower-like nanospheres can be fine-tuned. Both the depth and the opening diameter of the cone-like cavities can be regulated from 40 to 2 nm by controlling the polymerization of butyraldehyde during the synthesis process, simultaneously, the smaller mesopores in the cone-like cavity wall become more ordered. To the best of our knowledge, this is the first report on the fine tuning of the hierarchical pore structure of the flower-like silica nanospheres.

Experimental

Materials

Tetraethyl orthosilicate (TEOS) (99 wt%) and cetyltrimethylammonium bromide (CTAB) (99.9 wt%) were obtained from Tianjin Fine Chemical Institute. Aqueous ammonia (NH4OH) (25-28 wt%) was purchased from Shantou Xilong Chemical Factory. Acetaldehyde solution, propionaldehyde, butyraldehyde and amyl aldehyde were purchased from Sinopharm Chemical Reagent Co., Ltd., China. Deionized water was prepared in our laboratory. All chemicals were analytical grade and were used as received without any further purification.

Preparation of hierarchical porous silica nanospheres

The hierarchical porous silica nanospheres were prepared by the modified Stöber method in the TEOS-CTAB-NH3•H2O-aldehyde system. For the typical synthesis of micro/mesoporous silica nanospheres, 0.64 g of CTAB, 15 ml of acetaldehyde solution (40 wt%), and 12 ml of water were mixed in a 100 ml closed flask and stirred at 27 °C for 5 min. Then 2.8 ml of NH_4OH (25-28 wt %) was quickly added to the mixture. After stirring for 30 min, 2.8 ml of TEOS was added into the mixture. The mixture was further stirred vigorously for 24 h. The resulting mixture was brown, and the product was filtered, washed with deionized water and dried at 60 °C overnight. In the TEOS-CTAB-NH_3•H2O-propionaldehyde, butyraldehyde or amyl aldehyde system, flower-like hierarchical porous silica nanospheres were synthesized. The template and other organic components were removed by calcination in air at 540 °C for 6 h, white products were obtained. The samples were named as S-n- x (n：sample number; x: the aldehyde used, A-Acetaldehyde, P--Propionaldehyde, B-Butyraldehyde). The molar ratios of the reactants aldehyde: H_2O: CTAB: NH_3: TEOS were x: 100: 0.14: y: 1.The molar ratio of aldehyde, pH of the synthesis solution and the particle size of the samples are shown in Table 1.

Table 1. Molar ratios of reactants for the synthesis of hierarchical porous silica nanospheres

Sample	A/W ratio[a]	Initial pH	AD (nm) [b]	T (°C)[c]	S (m^2g^{-1})[d]	P (cm^3g^{-1})[e]
S-1-A	0.11	9.1	71	27	793	1.79
S-2-A	0.13	8.8	149	27	658	1.44
S-3-A	0.17	8.0	314	27	636	0.89
S-4-A	0.22	7.6	850	27	610	0.53
S-5-A	0.17	7.6	380	27	---	---
S-6-A	0.17	8.5	164	27	---	---
S-7-A	0.17	9.4	68	27	---	---
S-8-A	0.17	10.4	40	27	---	---
S-9-A	0.22	8.5	335	27	---	---
S-10-A	0.11	8.5	95	27	---	---
S-11-P	0.11	9.0	120	27	826	0.78
S-12-B	0.11	9.0	120	27	628	2.34
S-13-A	0.11	9.1	210	85	807	0.72
S-14-A	0.11	9.1	—	100	785	0.75
S-15-B	0.11	9.0	130	85	610	1.22
S-16-B	0.11	9.0	150	100	608	0.82

[a]A/W ratio: the molar ration of aldehyde to water

[b] AD--Average diameter. Obtained by measuring at least 100 individual particles on the SEM image of each sample.

[c]T— Synthesis temperature. [d]S—specific surface. [e]P—Pore volume.

Characterization

Powder X-ray diffraction (XRD) measurements were performed on a Rigaku D/Max 2400 diffractometer with Cu Kα radiation. Scanning electron microscopy (SEM) images were obtained on a Hitachi S-4800 implement. Some samples were sputtered with a thin film of gold. Transmission electron microscopy (TEM) images were recorded on a Tecnai G2 20 S-twin instrument (FEI Company) with an acceleration voltage of 200 kV. The samples for TEM analysis were prepared by dipping carbon-coated copper grids into ethanol solutions of silica and drying at ambient condition. Nitrogen sorption isotherms were obtained using a Quanta chrome Autosorb-1-MP apparatus at liquid nitrogen temperature. Prior to the measurements, the samples were degassed at 300 °C overnight. The specific surface areas were calculated from the adsorption data in the relative pressure intervals from 0.04 to 0.2 by the Brunauer-Emmett-Teller (BET) method. Mesoporous size distribution curves were calculated by the Barrett-Joyner-Halenda (BJH) method from the adsorption branch. The microporous distribution was calculated by using SF method. The total pore volume was estimated from the amount adsorbed at the relative pressure of 0.99. TG analysis was conducted on a TGA/SDTA851e thermo-balance (Mettler Toledo). The thermal analysis data were collected in the range of 308-1173 K in an air flow. The heating rate was 10 K min^{-1} at a flow rate of 25 ml min^{-1} while the sample weight was between 7 and 10 mg.

Results and discussion

Size-controlled micro/mesoporous silica nanospheres synthesized with acetaldehyde

Size-controlled micro/mesoporous silica nanospheres (MMSNs) were successfully synthesized in the TEOS-CTAB-NH_3•H2O-acetaldehyde system by the aldehyde-modified Stöber method. The molar ratios of the aldehyde to water (A/W R), the pH of the synthesis solution and synthesis temperature are shown in Table 1. The surface of the MMSNs synthesized with acetaldehyde is smooth and the particle size can be regulated by changing A/W R. The average diameters of the synthesized samples using acetaldehyde increased with increasing A/W R in the order of 71 nm (R=0.11), 149 nm (R=0.13), 314 nm (R=0.17), and 850 nm (R=0.22), as shown in Figure 1a-d, respectively. Figure S1 shows the diameter distribution of MMSNs synthesized with different A/W R in the Electronic Supplementary Information (ESI).

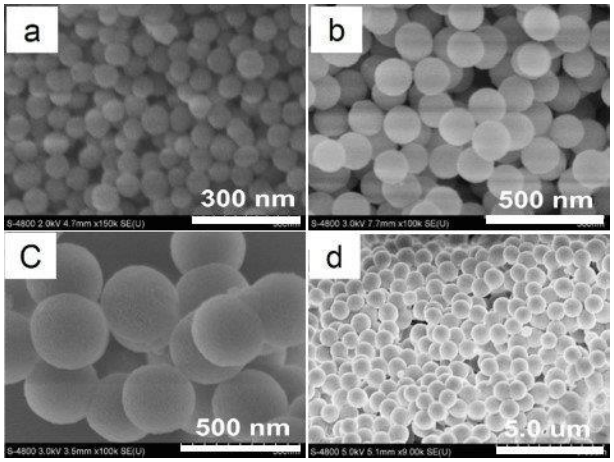

Figure1. SEM images of MMSNs synthesized with different A/W at 27 oC: (a) S-1-A (R=0.11), (b) S-2- A (R=0.13), (c) S-3- A (R=0.17), and (d) S-4-A (R=0.22).

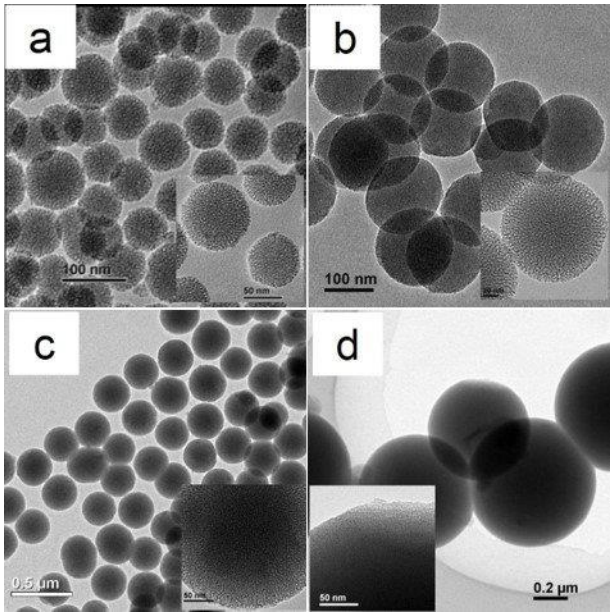

Figure 2. TEM images of MMSNs synthesized with different A/W at 27 °C: (a) S-1- A (R=0.11), (b) S-2- A (R=0.13), (c) S-3- A (R=0.17), and (d) S-4- A (R=0.22).

The TEM images of the MMSNs also confirmed that the monodisperse silica nanosphere diameter increased from about 70 nm to 1.0 um with the increasing A/W R (Figure 2 a-d), which is in agreement with the SEM images. The silica nanospheres become more uniform with the increasing size (Figure 2c). Higher magnification TEM images (the inset) show that worm-like mesopores are in all of the samples.

The XRD patterns of the samples with different A/W R all show a broad diffraction peak at ca.2° (Figure 3A), which indicates worm-like mesopores in the silica nanospheres[34]. The result is consistent with the TEM images. Nitrogen adsorption-desorption isotherms of the samples are shown in Figure 3B. All the nitrogen sorption isotherms of the samples show an abrupt adsorption of nitrogen at low relative pressures (P/P_0<0.01), which suggests the presence of micropores in the silica nanospheres. The SF pore size distribution analysis revealed that the micropore distribution is around 0.54-0.58 nm (Figure S2). The capillary condensation of N_2 at the relative pressure P/P_0 from 0.2 to 0.4 suggests mesopores in the silica nanospheres. The mesopore diameter is about 2-4 nm calculated from the adsorption branch by BJH method (Figure S2). With the increasing A/W R, the capillary condensation of N_2 at high relative pressure ($P/P_0 > 0.9$) decreases due to the increasing particle size of the MMSNs.

The particle size of the MMSNs can be affected by the initial pH which influences the hydrolysis and condensation processes of TEOS[35]. During the synthesis of the MMSNs with different A/W R, the initial pH of the synthesis system is different because the acetaldehyde solution is acidic (Table 1). To investigate the influence of initial pH on the particle size, MMSNs was synthesized at different pH with the same A/W R=0.17. The average sphere diameter decreased with the increasing pH in the order of 380 (pH =7.6), 164(pH =8.5), 68 (pH =9.4) and 40 nm (pH =10.4), as shown in figure 4 a-d, respectively. Smaller silica nanospheres were formed when the initial pH of the reaction solution was higher, because the net charge of OH^- prohibits new silicate anions to join the silica particles which precipitate in the synthesis system[35]. The silica nanosphere diameter distributions of the MMSNs synthesized at different initial pH are in ESI Figure S3.

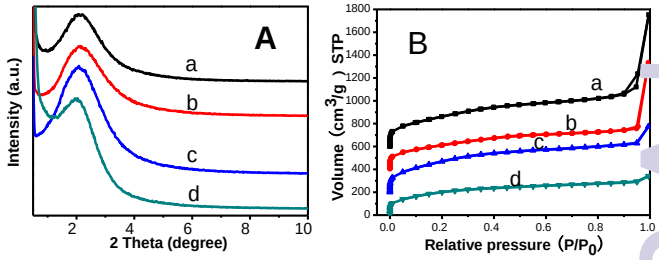

Figure3. XRD patterns (A) and Nitrogen adsorption-desorption isotherms (B) of MMSNs synthesized with different A/W at 27 °C : (a) S-1-A (R=0.11), (b) S-2-A (R=0.13), (c) S-3-A (R=0.17), and (d) S-4-A (R=0.22).

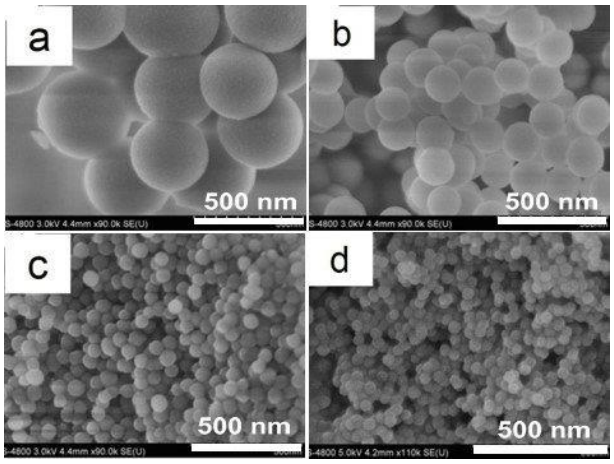

Figure 4. SEM images of MMSNs synthesized at different initial pH with the same A/W R=0.17: (a) S-5-A (pH=7.6), (b) S-6- A (pH=8.5), (c) S-7- A (pH=9.4), and (d) S-8- A (pH=10.4).

To investigate the role of acetaldehyde during the synthesis of the MMSNs, samples with different A/W R were synthesized at pH=8.5 which were fine-tuned by ammonium. The SEM images show that the average sphere diameter decreased with the decreasing of A/W R in the order of 335 (R=0.22), 164 (R=0.17) and 95 nm (R =0.11), as shown in figrure 5 a-c, respectively. The diameter distributions of the MMSNs are shown in ESI Figure S4.

Both the initial pH of the synthesis solution and the concentration of acetaldehyde strongly affect the particle size. Regulating the pH of the synthesis solution and the A/W R can fine tune the MMSN diameter from 40 to 850 nm.

Flower-like hierarchical porous silica nanospheres synthesized with propionaldehyde or butyraldehyde

Flower-like hierarchical porous silica nanospheres were synthesized in the TEOS-CTAB-NH_3•H_2O-propionaldehyde or butyraldehyde system by the modified Stöber method. The silica nanospheres exhibit cone-like cavities in the surface (Figure 6). All the cone-like cavities are open

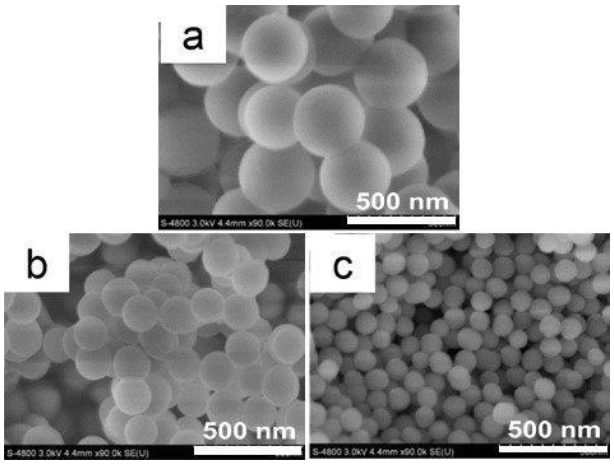

Figure 5. SEM images of MMSNs synthesized with different A/W R at the initial pH =8.5: (a) S-9- A (R=0.22), (b) S-6- A (R=0.17), and (c) S-10- A (R =0.11)

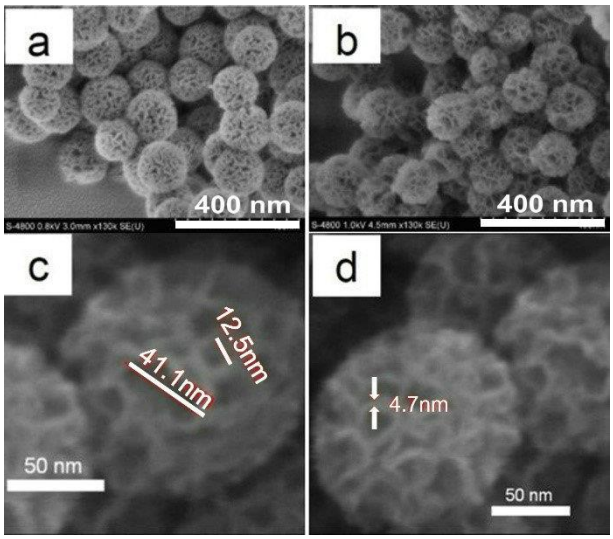

Figure 6. SEM images of MMSNs: (a) S-11- P, (b, c, d) S-12- B

and the cavity opening diameter of sample S-12-B is larger than that of S-11-P (Figure 6 a, b). Higher magnification SEM images of S-12-B show that the cavity opening diameter is between 12.5 to 41.1 nm (Figure 6 c), and the thickness of the cone-like cavity wall is about 4.7 nm (Figure 6 d). The diameter of the flower-like hierarchical porous silica nanosphere is less than 130 nm (Figure 6 a, b). The TEM images of S-11-P and S-12-B also show that both the samples are flower- like silica spheres, the diameter of S-12-B is about 120 nm and a little smaller than that of S-11-P which is about 130 nm (Figure 7 a, b). Cone-like cavities are in the nanospheres from the core to the surface along the radius. The cone-like cavity opening diameter of S-12-B is larger than that of S-11-P, which is in agreement with the SEM image. And the cone-like cavity depth of the S-12-B is deeper than that of S-11-P.

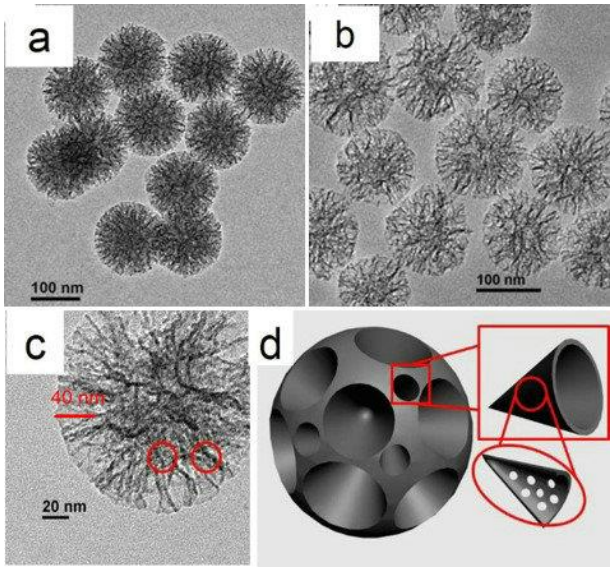

Figure 7. TEM images of MMSNs. (a) S-11-P, (b, c) S-12-B, and (d) Scheme of the hierarchical porous sphere.

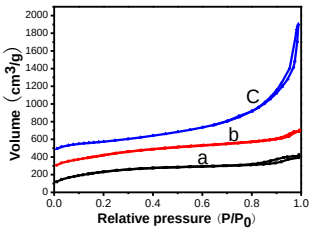

Figure 8. Nitrogen adsorption-desorption isotherms of FHMSNs synthesized with different aldehydes: (a) S-4-A, (b) S-11-P, and (c) S-12-B

Higher magnification TEM images of S-12-B show that there are small mesopores about 2-4 nm in the wall of the cone-like cavities (Figure 7c). Based on the results above, the structure of the flower-like hierarchical porous silica nanopheres is presented in Figure 7 d, the cone-like cavities with depth of ~ 40 nm and the mesopores of about 2-4 nm in the cavity wall constitute the hierarchical porous structure of the flower-like silica nanospheres.

XRD patterns of S-11-P and S-12-B are shown in FigureS5. The broad diffraction peak of both samples at ca. 2° suggests worm-like mesopores in the flower-like silica nanospheres. The nitrogen adsorption-desorption isotherms of S-11-P and S-12-B exhibit small increase in uptake of N_2 at the relative pressure P/P_0 ranging from 0.2 to 0.4, which also suggests the presence of mesopores (Figure 8 b, c). The pore size distribution of S-11-P is narrow and about 2.3 nm calculated from the adsorption branches by BJH method (ESI Figure S6). The nitrogen adsorption-desorption isotherms of S-12-B show an obvious uptake of N_2 at the relative pressure P/P_0 ranging from 0.8 to 1.0, which suggests large mesopores in the samples, namely, the cone-like cavities in the nanospheres. The pore size distribution of S-12-B is broad, which had a peak at about 2.8 nm and other pore distribution is from 4 to 40 nm (ESI Figure S6). The mesopores of 2.8 nm could be made by CTAB, and the larger broad pore distribution is due to the cone-like cavities in the nanospheres, which is consistent with the TEM results. When propionaldehyde is replaced by butyraldehyde during the synthesis process, the pore volume of the flower-like silica nanospheres increases from 0.78 to 2.34 $cm^3.g^{-1}$, while the BET surface area decreases from 826 to 628 $m^2.g^{-1}$. All these results above prove that the flower-like hierarchical porous silica nanospheres is constituted by the large cone-like cavities and small mesopores in the cavity wall.

Fine tuning of the hierarchical pore structure of the silica nanospheres

The hierarchical pore structure of the silica nanospheres can be fine-tuned by the synthesis temperature. For MMSNs synthesized with acetaldehyde at the same reactant molar ratio, both the mesopore structure and particle size can be regulated by the synthesis temperature. Figure 9 shows typical TEM images of sample S-13-A and S-14-A which were synthesized at 85 °C and 100 °C, respectively. The diameter of S-13-A is about 210 nm (Figure 9 a) and worm-like mesopores is obvious in the

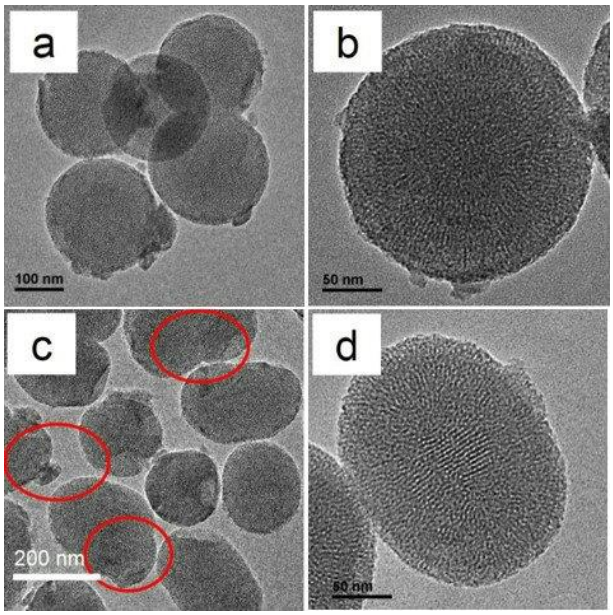

Figure 9. TEM images of MMSNs synthesized at different temperature. (a,b) S-13- A 85 °C and (c,d) S-14- A 100 °C

silica nanospheres (Figure 9 b). Increasing the synthesis temperature to 100 °C, some of the silica nanospheres grow together and turn into elongated nanoparticles (Figure 9 c). As a consequence, the length of the elongated nanoparticles is about 300 nm. The mesopore channels in the silica nanospheres are clearer (Figure 9 d), which indicates the mesopores in S-14-A is more ordered. As comparison, the diameter of S-1-A which was synthesized at 27 °C with the same reactant molar ratio is about 71 nm (Figure 1a), and the mesopores in the nanospheres is less ordered (Figure 2a). The SEM images of the samples synthesized at 85 °C and 100 °C also confirm the growth of the silica nanospheres and the aggregations between silica spheres with the increasing of the synthesis temperature (ESI Figure S7). The XRD patterns of sample S-13-A and S-14-A show narrower diffraction peak at about ca.2° (Figure10), which suggest more ordered of the mesopores in the samples than that of mesopores in sample S-1-A. The result is in agreement with the TEM images.

The nitrogen adsorption-desorption isotherms and pore size distributions of S-13-A and S-14-A are shown in Figure11. Compared to that of S-1-A, there are obvious capillary condensation of N_2 at the relative pressure P/P_0 ranging from 0.2 to 0.4, which suggests there are more mesopores in both samples of S-13-A (Figure 11 A a) and S-14-A (Figure 11 A b). The mesopore diameter is about 2.7 nm

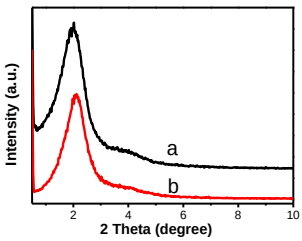

Figure10. Powder XRD patterns for MMSNs synthesized at different temperatures: (a) S-13-A 85 °C and (b) S-14-A 100 °C.

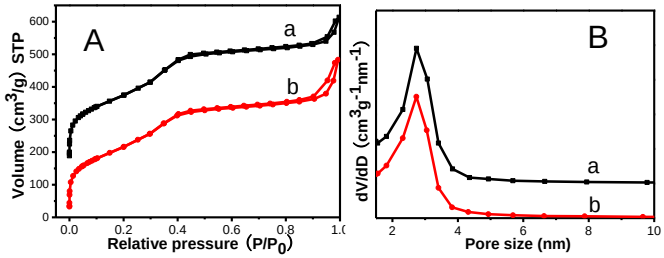

Figure11. Nitrogen adsorption-desorption isotherms and pore size distributions of MMSNs synthesized at different temperatures: (a) S-13-A 85 °C and (b) S-14-A 100 °C

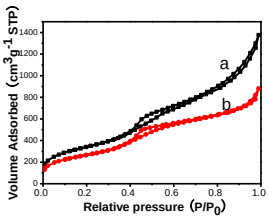

Figure 13. Nitrogen adsorption-desorption isotherms of MMSNs synthesized at different temperatures: (a) S-15-B 85 °C and (b) S-16-B 100 °C

calculated from the adsorption branch by BJH method (Figure 11 B).

The hierarchical pore structure of the flower-like silica nanospheres can also be fine-tuned by the synthesis temperature. The SEM images (Figure 12 a, b) show the silica nanospheres of sample S-15-B and S-16-B which were synthesized at 85 and 100 °C, respectively. The cone-like cavity depth of S-15-B is deeper than that of S-16-B in the silica spheres. The TEM images also show that the flower-like hierarchical porous silica nanospheres synthesized at different temperature are monodisperse and uniform (Figure 12 c, e). The cone-like cavity depth of S-15-B is about 25 nm (Figure 12 d), with the increasing of the synthesis temperature to 100 °C, the cone-like cavities are not obvious (Figure 12 f). Compared to the cone-like cavity depth of ~40 nm in

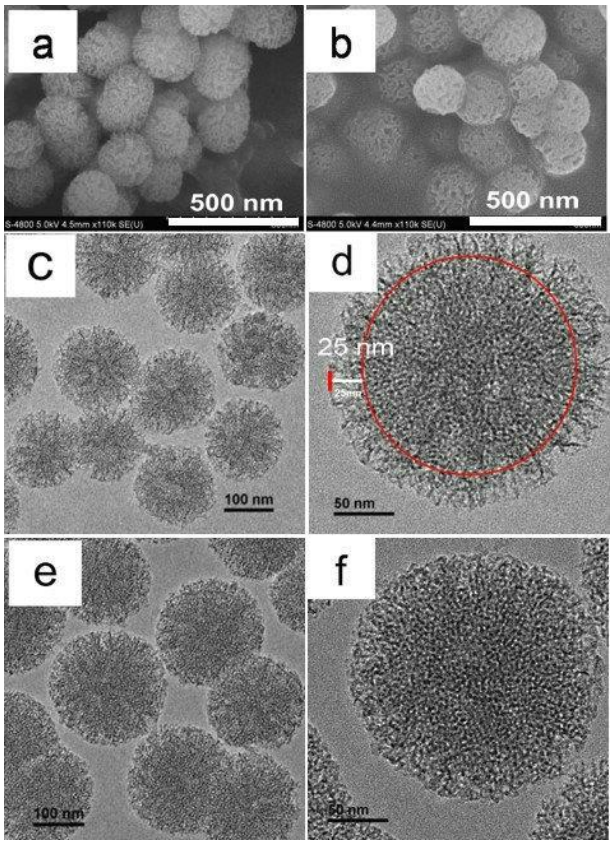

Figure12. SEM and TEM images of S-15-B (a, c, d 85 °C) and S-16-B (b, e, f 100 °C).

S-12-B (Figure 7 c), it can be seen that the depth of the cone-like cavities along the radial direction decreases with the increasing of the synthesis temperature gradually. Correspondingly, the diameter of the cone-like cavity opening also decreases to no more than 20 nm in S-15-B synthesized at 85 °C (Figure 12 d), and nearly disappears in the S-16-B synthesized at 100 °C (Figure 12f). However, the smaller mesopores templated by CTAB are clearer in the TEM images (Figure 12 d, f), compared to that of S-12- B (Figure 7 a-c).

Nitrogen adsorption-desorption isotherms of S-15-B and S-16-B are shown in Figure 13. Compared to the sample of S-12-B synthesized at 27 °C (Figure 8 c), there are obvious capillary condensation of N_2 at the relative pressure P/P_0 ranging from 0.2 to 0.4, which suggests more mesopores in the nanospheres synthesized at higher temperature. However, the uptake of N_2 at the relative pressure P/P_0 ranging from 0.8 to 1.0 is lower than that of S-12-B, especially for the S-16-B. The pore volume of S-12-B, S-15-B and S-16-B is 2.34, 1.22 and 0.82 cm^3g^{-1}, respectively, which also indicates the decreasing of the cone-like cavities with the increasing of the synthesis temperature. The results are consistent with the SEM and TEM images. From the results above, it can be seen that the hierarchical pore structured of the flower-like silica nanospheres can be fine tuned by regulating the synthesis temperature.

Synthesis mechanism

In our previous work[14], silica nanospheres of about 30 nm were obtained and formaldehyde was used as suppressant which formed a polymer shell on the outer surface of the nanospheres, suggesting the polymerization of aldehyde in the synthesis process. For the synthesis of MMSNs, acetaldehyde affects the hydrolysis and condensation processes of TEOS, which resulted in the regulation of the particle size by tuning the A/W R. However, acetaldehyde is difficult to form polymer at the temperature above its freezing point (-123.5 °C) [36, 37]. At the synthesis temperature of 27 °C, acetaldehyde oligomer may be obtained, which act as template to form micropores in the MMSNs. The TG/DTG curves of the S-1-A precursor are shown in Figure 14. The sample displays a weight loss around 100 due to the removal of physically adsorbed water. The subsequent weight losses around and 210 °C and 350 °C may be attributed to the removal of CTAB and acetaldehyde oligomer, respectively,

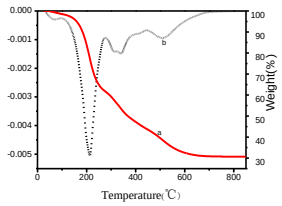

Figure 14. TG (solid line, a) and DTG (broken line, b) curves of S-1-A precursor.

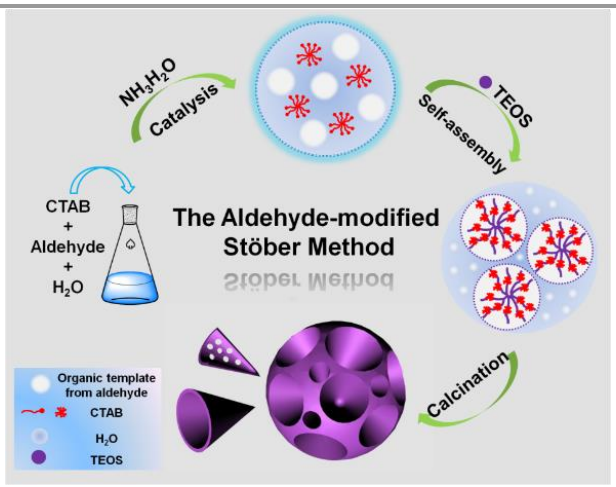

Scheme1. Synthesis mechanism of hierarchical porous silica nanospheres by the aldehyde-modified Stöber method

To further confirm the formation of aldehyde polymer or oligomer during the synthesis of hierarchical porous silica nanospheres, experiments were designed that all the synthesis reactants except tetraethyl orthosilicate were mixed and reacted at 27 °C. The acetaldehyde system is a clear brown sol, propionaldehyde system is yellow emulsion, and butyraldehyde system is a mixture of oil phase and water. Figure S8 A, B, C shows the GC-MS spectra of acetaldehyde, propionaldehyde system and the oil phase of butyraldehyde system, respectively. The results confirm that aldehyde oligomer or polymer are formed during the synthesis process. And the oligomers or polymers resulted in the formation of micropores or cone-like mesopores in the hierarchical porous silica nanospheres. Further increasing the chain length of the aldehyde to amyl aldehyde during the synthesis of hierarchical porous silica nanospheres, over blooming flower-like silica nanospheres were obtained and some nanospheres are worn-out (Figure S9). Based on the results above, the scheme of the synthesis of hierarchical porous silica nanospheres by the aldehyde-modified Stöber method is proposed as Scheme 1.

Compared to the simultaneous polymerization of styrene into polystyrene during the synthesis of flower-like silica nanospheres[29], the simultaneous polymerization of acetaldehyde, propionaldehyde or butyraldehyde can be fine-tuned by the synthesis temperature. High temperature prohibits the aldehyde to form large polymer molecules[36, 37]. With the increasing temperature during the preparation of MMSNs, less or no acetaldehyde oligomers formed, the influence of which on the formation of mesopores templated by CTAB decreases, and mesopores become more ordered. During the synthesis of hierarchical porous flower-like silica nanospheres, large polymers or small oligomers of butyraldehyde are formed depending on the synthesis temperature, which resulted in the fine tuning of the hierarchical pore structure of the flower-like silica nanospheres. When the synthesis temperature is raised to 100 °C, little butyraldehyde oligomers are formed, which also results in the more ordered mesopores templated by CTAB.

Conclusions

In summary, hierarchical porous silica nanospheres with controlled size and fine-tuned pore structure were successfully prepared by the aldehyde-modified Stöber method. When acetaldehyde was used as a co-solvent, micro/mesoporous silica nanospheres were synthesized, the diameter of which can be controlled from 40 to 850 nm by regulating the molar ratio of acetaldehyde to water and the initial pH of the synthesis solution. Increasing the synthesis temperature increased the diameter of the silica spheres and the mesopores in the spheres become more ordered. When propionaldehyde or butyraldehyde was used as a co-solvent, flower-like hierarchical porous silica nanospheres with large cone-like cavities and mesopores in the cavity wall were synthesized. Both the depth and the diameter of the cone-like cavity can be fine-tuned from 40 to 2 nm by increasing the synthesis temperature from 27 to 100 °C, simultaneously, the mesopores in the cone-like cavity wall become more ordered. These size-controllable and mesostructure-tunable hierarchical porous silica nanospheres have potential applications in the fields of catalytic materials, nano- and bio-medicine, and nanodevices as well as other applications involving large molecules.

Acknowledgements

This work was financially supported by the National Natural Science Foundation of China 21306018.

References

1. Z. Zhu, RSC Adv, 2015, 5, 28624-28632.
2. N. Saman, K. Johari and H. Mat, Clean Technologies and Environmental Policy, 2015, 17, 39-47.
3. Y.-P. Zhu, Y.-L. Liu, T.-Z. Ren and Z.-Y. Yuan, Nanoscale, 2014, 6, 6627-6636.
4. F. Wang, Y. Tang, B. Zhang, B. Chen and Y. Wang, *J Colloid Interf Sci*, 2012, **386**, 129-134.
5. M. Shokouhimehr, Y. Piao, J. Kim, Y. Jang and T. Hyeon, *Angewandte Chemie*, 2007, **46**, 7039-7043.
6. C. Jin, Y. Wang, H. Wei, H. Tang, X. Liu, T. Lua and J. Wang, *J Mater Chem A*, 2014, **2**, 11202-11208.
7. C. Y. Lai, B. G. Trewyn, D. M. Jeftinija, K. Jeftinija, S. Xu, S. Jeftinija and V. S. Y. Lin, *J Am Chem Soc*, 2003, **125**, 4451-4459.
8. G. D. S. Leirose and M. B. Cardoso, *Journal of Pharmaceutical Sciences*, 2011, **100**, 2826-2834.
9. J. Lu, M. Liong, J. I. Zink and F. Tamanoi, *Small*, 2007, **3**, 1341-1346.
10. Y. Zhu, J. Shi, W. Shen, X. Dong, J. Feng, M. Ruan and Y. Li,

Angewandte Chemie, 2005, **44**, 5083-5087.
11. I. I. Slowing, B. G. Trewyn, S. Giri and V. S. Y. Lin, *Advanced Functional Materials*, 2007, **17**, 1225-1236.
12. J. M. Rosenholm, E. Peuhu, L. T. Bate-Eya, J. E. Eriksson, C. Sahlgren and M. Linden, *Small*, 2010, **6**, 1234-1241.
13. J. M. Rosenholm, A. Meinander, E. Peuhu, R. Niemi, J. E. Eriksson, C. Sahlgren and M. Linden, *ACS Nano*, 2009, **3**, 197-206.
14. L. Gu, A. F. Zhang, K. K. Hou, C. Y. Dai, S. Zhang, M. Liu, C. S. Song and X. W. Guo, *Micropor Mesopor Mat*, 2012, **152**, 9-15.
15. K. Suzuki, K. Ikari and H. Imai, *J Am Chem Soc*, 2004, **126**, 462-463.
16. K. Moeller, J. Kobler and T. Bein, *Advanced Functional Materials*, 2007, **17**, 605-612.
17. C. Urata, Y. Aoyama, A. Tonegawa, Y. Yamauchi and K. Kuroda, *Chem Commun*, 2009, 5094-5096.
18. K. Cheng and C. C. Landry, *J Am Chem Soc*, 2007, **129**, 9674-9685.
19. N. Suriyanon, P. Punyapalakul and C. Ngamcharussrivichai, *Mater Chem Phys*, 2015, **149**, 701-712.
20. C. E. Fowler, D. Khushalani, B. Lebeau and S. Mann, *Adv Mater*, 2001, **13**, 649-652.
21. D.-C. Guo, W.-C. Li, W. Dong, G.-P. Hao, Y.-Y. Xu and A.-H. Lu, *Carbon*, 2013, **62**, 322-329.
22. W. Stöber, A. Fink, E. Bohn, *J. Colloid Interface Sci.* **1968**, 26, 62– 69.
23. T. Martin, A. Galarneau, F. Di Renzo, F. Fajula and D. Plee, *Angew Chem Int Edit*, 2002, **41**, 2590-2592.
24. P. Botella, A. Corma and M. T. Navarro, *Chem Mater*, 2007, **19**, 1979-1983.
25. S. Lim, A. Ranade, G. Du, L. D. Pfefferle and G. L. Haller, *Chem Mater*, 2006, **18**, 5584-5590.
26. H. Zhang, Z. Li, P. Xu, R. Wu and Z. Jiao, *Chem Commun*, 2010, **46**, 6783-6785.
27. J. Huang, X. Xu, C. Gu, G. Fu, W. Wang and J. Liu, *Mater Res Bull*, 2012, **47**, 3224-3232.
28. X. Du and J. He, *Langmuir*, 2010, **26**, 10057-10062.
29. A. B. D. Nandiyanto, S.-G. Kim, F. Iskandar and K. Okuyama, *Micropor Mesopor Mat*, 2009, **120**, 447-453.
30. V. Polshettiwar, D. Cha, X. Zhang and J. M. Basset, *Angewandte Chemie*, 2010, **49**, 9652-9656.
31. C. Jin, J. Wang, Y. Wang, H. Tang and T. Lu, *J Sol-Gel Sci Techn*, 2014, **70**, 53-61.
32. K. Zhang, L. L. Xu, J. G. Jiang, N. Calin, K. F. Lam, S. J. Zhang, H. H. Wu, G. D. Wu, B. Albela, L. Bonneviot and P. Wu, *J Am Chem Soc*, 2013, **135**, 2427-2430.
33. H. Yang, S. Liao, C. Huang, L. Du, P. Chen, P. Huang, Z. Fu and Y. Li, *Appl Surf Sci*, 2014, **314**, 7-14.
34 H. Guo, F. Ye and H. Zhang, *Mater Lett,* 2008, **62**, 2125-2128.
35. Z.-A. Qiao, L. Zhang, M. Guo, Y. Liu and Q. Huo, *Chem Mater*, 2009, **21**, 3823-3829.
36. J. Furukawa, T. Saegusa, T. Tsuruta, H. Fujii and T. Tatano, *Journal of Polymer Science*, 1959, **36**, 546-546.
37. B. Q. Mao, Q. G. He, *Chemistry,* 1964, **1**, 17-26.